Nonlinear optics in germanium mid-infrared fiber material: Detuning oscillations in femtosecond mid-infrared spectroscopy

Cite as: AIP Advances **7**, 095125 (2017); https://doi.org/10.1063/1.5003027
Submitted: 01 September 2017 . Accepted: 19 September 2017 . Published Online: 28 September 2017

M. Ordu, J. Guo, G. Ng Pack, P. Shah, S. Ramachandran, M. K. Hong, L. D. Ziegler, S. N. Basu, and S. Erramilli

Nonlinear optics in germanium mid-infrared fiber material: Detuning oscillations in femtosecond mid-infrared spectroscopy

M. Ordu,[1] J. Guo,[2] G. Ng Pack,[3] P. Shah,[3] S. Ramachandran,[2,4,5] M. K. Hong,[5,6] L. D. Ziegler,[3,5] S. N. Basu,[1,2,5,a] and S. Erramilli[5,6,7,a]
[1]*Department of Mechanical Engineering, Boston University, Boston, Massachusetts 02215, USA*
[2]*Division of Materials Science and Engineering, Boston University, Brookline, Massachusetts 02446, USA*
[3]*Department of Chemistry, Boston University, Boston, Massachusetts 02215, USA*
[4]*Department of Electrical and Computer Engineering, Boston University, Boston, Massachusetts 02215, USA*
[5]*Photonics Center, Boston University, Boston, Massachusetts 02215, USA*
[6]*Department of Physics, Boston University, Boston, Massachusetts 02215, USA*
[7]*Department of Biomedical Engineering, Boston University, Boston, Massachusetts 02215, USA*

(Received 1 September 2017; accepted 19 September 2017; published online 28 September 2017)

Germanium optical fibers hold great promise in extending semiconductor photonics into the fundamentally important mid-infrared region of the electromagnetic spectrum. The demonstration of nonlinear response in fabricated Ge fiber samples is a key step in the development of mid-infrared fiber materials. Here we report the observation of detuning oscillations in a germanium fiber in the mid-infrared region using femtosecond dispersed pump-probe spectroscopy. Detuning oscillations are observed in the frequency-resolved response when mid-infrared pump and probe pulses are overlapped in a fiber segment. The oscillations arise from the nonlinear frequency resolved nonlinear ($\chi^{(3)}$) response in the germanium semiconductor. Our work represents the first observation of coherent oscillations in the emerging field of germanium mid-infrared fiber optics. https://doi.org/10.1063/1.5003027

I. INTRODUCTION

Semiconductors are immensely attractive materials for transmission in the mid-infrared (IR) region due to their transparency and large refractive index. Given the importance of both mid-wave infrared and long-wave infrared regions for molecular spectroscopy for chemical and biological sensing,[1] hyperspectral imaging,[2] standoff detection,[3] mid-infrared astronomy[4] and astrophotonics,[5] considerable progress has been made in group IV infrared photonics using both silicon and germanium.[6–8] Ge is especially suitable for mid-infrared nonlinear optics because of its exceptionally high values of important nonlinear optical coefficients. Among the common dielectric materials and semiconductors, Ge with its small ~ 0.67 eV band gap has the highest linear refractive index of n ~ 4 as well as the highest nonlinear refractive index coefficient, with a Kerr coefficient $n_2 = 10^{-17}$ m^2/W that scales inversely with the band gap in accordance with the model of Sheik-Bahae et al.[9] Among common crystalline materials, Ge also has the highest third order susceptibility[10] $\chi^{(3)} = 1.5 \times 10^{-18}$ m^2/V^2 near 2500 cm^{-1} or at wavelengths near 4000 nm. The nonlinear properties of Ge and related materials have spurred interest in extending group IV photonics to the important longer wavelength

[a]Authors to whom correspondence should be addressed. Electronic mail: shyam@bu.edu, basu@bu.edu

regions of the infrared spectrum for both linear and nonlinear applications.[6] The pioneering work of Ballato and co-workers has opened up the scope of semiconductor Si-core and Ge-core fibers[11] as an alternative to chalcogenide glass fibers[12] for detailed characterization and evaluation for potential applications. Recently we have developed a scalable process using a relatively low drawing temperature in a custom-built draw tower to obtain Ge-core fibers with transmission losses of ~ 5 dB/cm in the mid-infrared fingerprint region.[13] Studies are focused on post fiber drawing/deposition processes to decrease the transmission losses.[14,15] An earlier study reported measurement of the Raman shift in Ge-core fibers arising from a vibrational normal mode in Ge.[16] Here we report the first nonlinear off-resonance optical material response in the Ge core of as-drawn fibers. The work lays the foundation for further developments in nonlinear mid-infrared optics in a fast emerging application field.

Detuning oscillations are a striking phenomenon associated with cross-coupling effects, and were first reported by Ziegler and collaborators[17,18] in the frequency-dispersed optical heterodyne nonlinear response of organic liquids due to incident ~ 35 fs laser pulses centered near 600 nm. In a related but different context, self-frequency detuning effects have been reported with visible lasers in phase-conjugate mirrors systems with counter propagating beams and ring oscillators based on photorefractive crystals originating from self-induced grating dynamincs.[19] Here we report four-wave mixing experiments on Ge fiber segments in femtosecond pump-probe spectroscopy using 90 fs Gaussian mid-infrared laser pulses centered at a carrier frequency of 2170 cm^{-1}. Detuning oscillations are observed in two-dimensional spectrograms when the signal wave is dispersed in frequency at varying delay intervals between the pump and probe pulse (Fig. 1(a)). The oscillations occur at the detuning frequency when pump and probe pulses interfere. In transparent materials, the oscillations do not correspond to molecular electronic or vibrational levels. Rather, they arise from the off-resonance electronic response in nonlinear optical materials,[18] and appear in frequency-dispersed optical heterodyne detection schemes, such as the standard pump-probe configuration. The observation of these oscillations is a signature of a general $\chi^{(3)}$ process associated with the third-order polarization $P^{(3)}$ response in a transparent material far from resonance. No particular requirement of lattice symmetry is needed, in contrast to frequency doubling, or parametric down-conversion processes, and the oscillations can be observed even in amorphous materials, liquids, and in centrosymmetric materials like Ge or Si in the mid-infrared as shown here.

Femtosecond four-wave mixing experiments arising from third-order nonlinear processes have spun off a rich set of multidimensional spectroscopic techniques in nonlinear optics.[20] These include photon echo,[21] third harmonic generation, transient grating, various forms of Raman spectroscopies, and 2D infrared spectroscopy.[22] Four-wave mixing begins with three incoming electric fields $\mathbf{E}_1(\mathbf{r},t)$, $\mathbf{E}_2(\mathbf{r},t)$, $\mathbf{E}_3(\mathbf{r},t)$. The interaction of the incoming modes in the nonlinear medium generates a nonlinear polarization field $\mathbf{P}(\mathbf{r},t)$ that acts as a source for a signal electric field $\mathbf{E}_s(\mathbf{r},t)$. The signal is measured in heterodyne detection, where the signal field is superposed with a local oscillator field, $\mathbf{E}_{LO}$. The detected intensity is proportional to $|\mathbf{E_s} + \mathbf{E}_{LO}|^2$ generating in the detected heterodyne

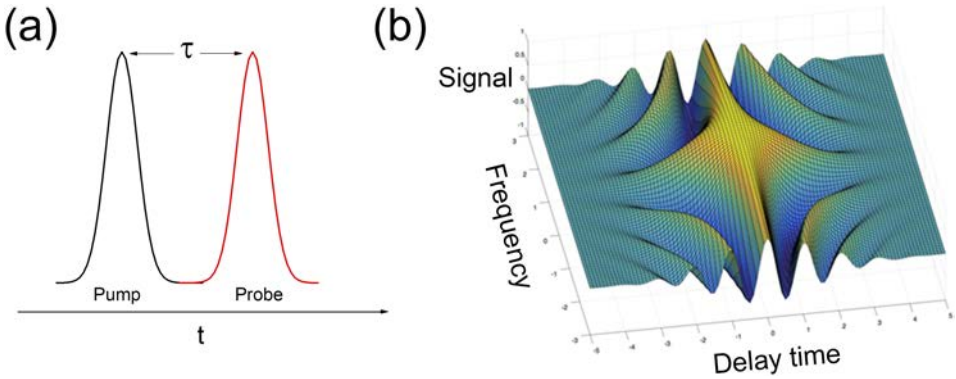

FIG. 1. (a) Time delay between the pump and the probe pulses. (b) Simulation of detuning oscillations, with the nonlinear signal shown in a surface plot versus the frequency and time delay.

signal intensity $S = \frac{\zeta}{2Z_0}\mathrm{Re}\left(\mathbf{E}_\mathbf{s}^* \cdot \mathbf{E}_{\mathrm{LO}}\right)$ that is linearly proportional to the signal polarization field. The proportionality constant includes a geometric experimental factor ζ derived from the constant transfer function between the exit face of the fiber and detector element, and Z_0, the free space impedance. Importantly, this phase-sensitive technique allows for determination of both the amplitude and phase of the polarization field. When the incoming waves are ultrafast, with temporal widths in the femtosecond scale, four-wave mixing experiments yield a rich superposition of the Fourier component modes as described below. In the pump-probe geometry used in our experiments, the electric field from the probe pulse serves as the local oscillator and the analysis is particularly straightforward.

II. MATERIALS AND METHODS

A. Fiber and microstructural characterization

10 mm long, 3 mm diameter Ge rods were core-drilled out of a 50×10×10 mm^3 monocrystalline Ge slab of 99.999% purity (Lattice Materials LLC, Bozeman, MT). Fiber preforms were made by placing a core-drilled Ge rod into a 3 mm inner diameter (ID) and 9 mm outer diameter (OD) borosilicate glass tube (Duran; Schott Glass, Germany). In order to prevent oxidation of the Ge during fiber drawing, the open ends on both sides of the Ge rod were sealed with 3 mm OD borosilicate glass rods of the same composition as the borosilicate glass tube. Fibers were drawn in a mini draw tower designed and assembled in-house at Boston University at 1000°C which is much lower than the typical silica fiber drawing temperature of 2000°C. More details of the fiber drawing process are presented elsewhere.[13,23]

Three drawn samples were chosen for this study: a cane with a 770 μm Ge core diameter, and two fibers with Ge core diameters of 132 μm and 358 μm respectively. All samples were imbedded into hardened epoxy and both sides of the samples were finely polished to a 0.05 μm surface finish by standard polishing procedures in order to improve facet quality.

Figure 2(a) shows a scanning electron microscope (SEM, Zeiss Supra 55, Germany) micrograph of a finely polished cross-section of a fiber with a 132 μm Ge-core diameter and 466 μm cladding diameter. The elemental composition profile across the core/cladding interface was obtained by a line-scan in the SEM along with energy dispersive x-ray spectroscopy (EDX; EDAX, NJ). The EDX elemental dot maps of Ge, Si and O are shown in Fig. 2(b)–(d). Figure 2(e) shows an EDX line scan through the core and cladding of the fiber marked by the orange line on the inset image, clearly indicating that the diffusion of oxygen and silicon from cladding to core is minimal. The low oxygen content of the core is likely due to the low processing temperature during the fiber drawing. This is

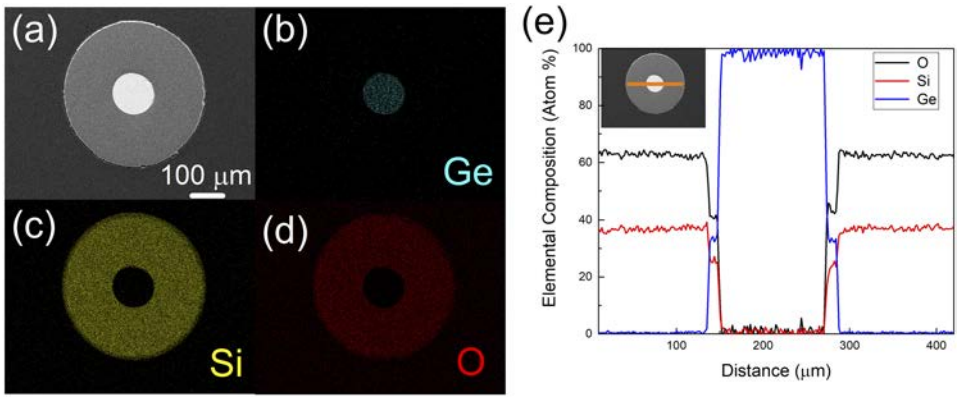

FIG. 2. (a) Scanning electron micrograph of the fiber sample. The Ge-core is the bright center, the glass cladding is the surrounding ring that is embedded in hardened epoxy. SEM-EDX elemental dot maps of (b) Ge, (c) Si and (d) O. (e) Composition profiles of Ge, Si and O derived from a line-scan, whose path is shown by a line in the inset SEM micrograph. The diffusion of elements across the interface is minimal.

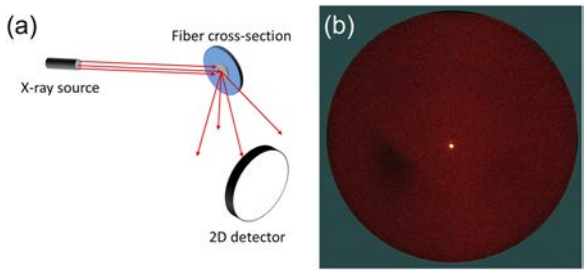

FIG. 3. (a) Schematic of 2D x-ray diffraction setup. (b) Reciprocal space mapping of the Ge core fiber with 1 mm diameter incident x-ray beam, showing a single (220) spot.

encouraging for the mid-IR transmission through the fiber for pump-probe spectroscopy since the oxygen is known to absorb mid-IR light.

Further the crystalline structure of Ge-core fiber were examined by x-ray diffraction spectroscopy (XRD; Bruker, Wisconsin). Reciprocal space mapping (RSM) of fiber core was carried out using a 1 mm diameter x-ray beam, using a 2D detector (Vantec, Bruker, Wisconsin). The schematic of the XRD setup is sketched in Fig 3(a). Figure 3(b) indicates that the scan consisted of a single (220) spot, indicating that the region in the Ge-core interrogated by the x-ray beam is a single crystal.

B. Femtosecond mid-IR pump-probe spectroscopy

Pump-probe experiments were performed on a 2DIR femtosecond system described elsewhere.[24] Mid-infrared femtosecond pulses were derived from a regeneratively amplified 800 nm 35 fs laser capable of operation at 7.5 mJ/pulse. Approximately 50% of this beam was sent to an Optical Parametric amplifier used to generate a signal and idler pulses in the near-infrared region. A home-built difference frequency generator was used to produce ~ 10 μJ tunable mid-infrared pulses. For this experiment, the carrier wave was tuned to ~ 2170 cm^{-1}, and the bandwidth was ~ 300 cm^{-1} associated with a pulse width of ~ 90 fs full-width-at-half-maximum (FWHM) operating at about 1.4× the transform limit. The spatial mode of the beam was Gaussian. The infrared beam was split into pump and probe pulses. A third beam for 2DIR studies was not used in the experiments reported here. The delay between pump and probe pulses was set by translating retroreflectors mounted on stepper motor controlled linear translation precision stages with 1 μm repeatability. The zero-crossings of the interference pattern resulting from co-propagating HeNe beams (632.8 nm) were used to determine the stage position and associated delay between pump and probe beams focused onto the input end of the Ge fiber sample using an off-axis paraboloid mirror. The generated third-order signal beam was collected from the output end using another off-axis paraboloid, dispersed by a monochromator and detected using a liquid-nitrogen cooled HgCdTe linear detector array. As stated before, the probe pulse serves as its own local oscillator with measurements of both amplitude and phase available in heterodyne detection.

III. DISCUSSION

A linearly polarized monochromatic wave traveling parallel to the z-axis corresponding to a particular Fourier component is described by an electric field $E_\omega(\omega,z)$ averaged over transverse coordinates.[25] Considering the ultrafast laser pulse as a superposition of monochromatic waves propagating in the z direction, the electric field averaged over a transverse coordinate is given by[25]

$$\frac{\partial E_\omega(\omega,z)}{\partial z} = \frac{i2\pi\omega}{cn_{eff}(\omega)} \int d\omega' \int d\omega'' \left[G(\omega,\omega',\omega'')\, E_\omega(\omega',z) \times E_\omega(\omega'',z) E_\omega{}^*(\omega'+\omega''-\omega,z)\, \chi^{(3)}(\omega-\omega') \exp(i\Delta kz)\right] \quad (1)$$

Equation (1) is the starting point for the textbook time-domain description where the propagation of light in nonlinear fiber optics is described by the nonlinear Schrodinger equation. In the time

domain, for a particular state of linear polarization, the third order response the electric field is given in a frame of reference set by the carrier wave by[25,26]

$$\frac{\partial E(z,t)}{\partial z} = -\frac{\alpha(\omega)}{2}E + i\sum_{m\geq 2}\frac{i^m\beta_m}{m!}\frac{\partial^m E}{\partial t^m} + i\gamma\left(1+\frac{i}{\omega_0}\frac{\partial}{\partial t}\right)\left[E(z,t)\int_{-\infty}^{+\infty}R(t')|E(z,t-t')|^2dt'\right] \quad (2)$$

The first term in Eq. (2) accounts for linear absorption, and higher order dispersion effects are described by the second term. The nonlinear response *R(t')* is assumed to be strictly local in space and independent of z, but will depend on past history. A detailed analysis for comparison with experiments is challenging. We assume that the response is far from any one-photon or two-photon absorption, and is primarily due to nonresonant electronic and nuclear degrees of freedom in the material. To check that the drawn fiber materials are indeed off-resonance with no sharp vibrational absorption bands, we have performed transmission measurements using a Quantum Cascade Laser (QCL) as well as a Fourier Transform infrared spectroscopy (FTIR) microscope as described in experimental section below. No sharp absorption bands were detected. In addition the pump and probe waves are also in a frequency range where two-photon absorption cross-section is also very low, with the 2-photon energy still well below the bandgap of Ge. We also assume that the local field approximation holds in the Ge fiber core and there are no long range correlations in the dielectric, in contrast for example to plasmonic metamaterial or photonic bandgap systems where there are spatial structures comparable to the scale of the wavelengths. Simplification of the analysis is also facilitated by using data from experiments performed with short sample lengths where we neglect higher order dispersion. Under these assumptions, Eq. (1) can then be readily integrated over z for each Fourier component, and the electric field at the end of the fiber of length of length L is then described in terms of an effective loss coefficient α_{eff} that is independent of the frequency over the narrow detuning range. The electric field amplitude then decays as $\sim E_{sZ}(t)e^{-\alpha_{eff}L/2}$ with the electric field $E_{sZ}(t)$ now described using the third order nonlinear response formalism described by Ziegler and co-workers. In the first theoretical analysis, the signal for detuning oscillations was derived in the Rotating Wave Approximation (RWA). To check against a potential inconsistency in adapting RWA to off-resonant nonlinear response, which is essentially instantaneous, off-resonant response is derived using the full four-wave mixing treatment. Mukamel has noted an issue concerning the use of the RWA to describe off resonant processes; a more rigorous analysis yields results that are indistinguishable from the observed experimental responses on the time scales probed in our infrared experiments.[20] The experiments measure the dispersed infrared signal that is the difference between the pump on vs pump off as described in the experimental section. This difference signal can be positive or negative depending on the time delay and the detuning frequency. Following Gardecki et al, the detected signal spectrograms are given by the following analytical expression that is symmetric with respect to the detuning Δ_D and the time delay t between the pump and probe pulses, and can be used to compare with the experimental data:

$$S(\Delta_D,t) = S_0 e^{-\alpha_{eff}L}\exp(-t^2/\tau_0^2)\exp(-\Delta_D^2/\Delta_0^2)\cos(f\Delta_D t+\phi) \quad (3)$$

Equation (3) is the central phenomenological result used to describe detuning oscillations. For identical incident Gaussian pulses, the parameter τ_0 describes the temporal width of the signal, while Δ_0 characterizes the width in frequency space. For a thin bulk transparent sample and transform limited identical Gaussian pulses, the parameters τ_0, Δ_0,f in Eq. (3) are related given by $\tau_0\Delta_0 = \frac{9}{2}$,$f = \frac{2}{3}$. For a thin sample, the phase shift ϕ is 0 or $\frac{\pi}{2}$ for dichroism and birefringence, respectively. For a long fiber sample, the phase shift is more general and appears as a shift of the apparent zero time delay point without affecting other parameters. The form and relations between the parameters depend on the shape of the pulses as shown in Gardecki et al.[18] For the fiber sample, with our laser pulses close to but not at the transform limit, although the parameters τ_0, Δ_D, f can in principle be calculated using microscopic model, they were varied independently to fit the data and to compare with the ideal values. Figure 1(b) shows a simulation that matches the observed periodicities in the detuning frequency as well the time delay. Equation (3) not only captures the essential symmetry between the

detuning Δ_D and the time delay t that is observed experimentally, but also the apparent time-reversal invariance between positive and negative time delays. This latter symmetry arises from the fundamental physical principle that when pump and probe beams overlap, the uncertainty principle and the indistinguishability of photons ensure that it is impossible to distinguish pump from probe beams. As

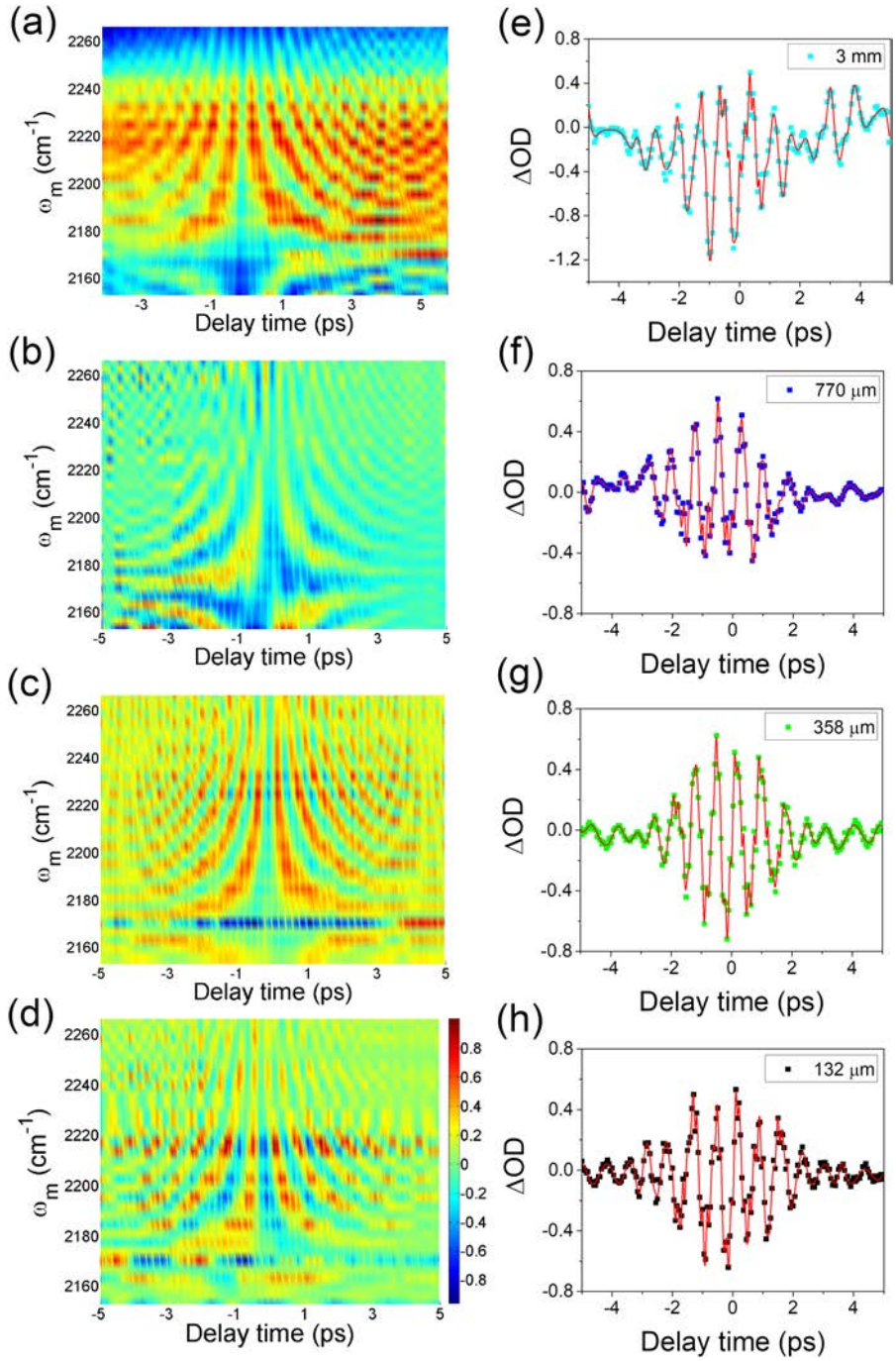

FIG. 4. Experimental results on four different samples: unprocessed Ge rod with 3 mm diameter, Ge cane with 770 μm-core diameter, Ge fiber with 358 μm-core diameter and Ge fiber with 132 μm-core diameter. (a), (b), (c) and (d) are contour plots of samples with respect to delay time (ps) and wavenumber (cm^{-1}). Each figures are individual from each other but have the same color code. Red indicates maximum normalized intensity whereas blue represents minimum normalized intensity. (e), (f), (g) and (h) show population decay of each sample with respect to delay time and optical delay difference at 2214 cm^{-1}.

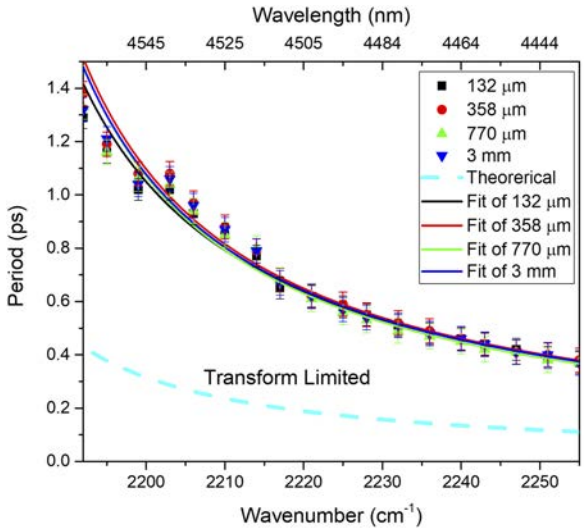

FIG. 5. Oscillation period as a function of frequency corresponding to different detuning values of four different samples with the following core diameters (i) 3mm Ge rod; (ii) 779 μm Ge cane; (iii) 132 μm and 358 μm Ge fibers.

is well known, a signal is observed even at negative time delays without of course violating causality, due to the finite non-zero electric field temporal widths of the laser beam pulses.

Figure 4 shows the experimental results from four different sets of samples. Figures 4(a)–(d) are surface plot with the colorized spectrogram signals as a function of time delay and dispersed frequency for four different samples ranging from a Ge fiber with 132 μm-core diameter to the starting unprocessed Ge 3 mm diameter rod. Figures 4(e)–(h) represent the corresponding data along a line cut at a selected frequency of 2214 cm^{-1} and shows the oscillations in the time domain that result from four-wave mixing. The period decreases with increasing detuning, as expected from Eq. (3).

Each of the time traces in Fig. 4 can be used to measure the period T of the dominant mode of oscillation as a function of detuning frequency Δ_D. Figure 5 shows a plot of the period for all the samples which is expected to a constant in the fitting model (Eq 3). The ratio of the parameters obtained from individual traces and global fitting are $\upsilon_0 = 2164 \pm 13, f = 31.5 \pm 0.5$ consistent with the detuning oscillation model used here. Figure 5 shows time traces at selected detuning frequencies. The period decreases with increasing detuning, as expected from Eq. (3).

IV. CONCLUSION

The salient features of the experimental results and detuning oscillations can only arise from nonlinear effects in the Ge material in the fiber. Nonlinear properties of Ge are maintained even after processing to form a fiber. Detuning oscillations are the signature of nonlinear response, observed in Ge fibers in the mid-infrared region for the first time. As the history of fiber optics demonstrates, with improved materials processing, and refinement with different cladding and coating materials, losses may be expected to reduce. Demonstration of nonlinear effects can be expected to have new applications in the mid-infrared region, such as optical switching, optical modulation and frequency generation.

ACKNOWLEDGMENTS

This work is supported in part by the National Science Foundation (NSF) through Grant No. CMMI-1301108. The authors would like to thank Dr. J. Bacon for assistance with the XRD studies.

[1] P. R. Griffiths and J. A. Haseth, *Fourier Transform Infrared Spectroscopy*, 2nd ed (Wiley, 2007).
[2] R. Bhargava, "Infrared spectroscopic imaging: The next generation," Appl Spectrosc. **66**(10), 1091–1120 (2012).
[3] C. K. N. Patel, "Single snapshot standoff detection using sub microsecond tuning speed quantum cascade lasers," Proc SPIE. **9836**, 98362E (2016).

[4] L. Labadie and O. Wallner, "Mid-infrared guided optics: A perspective for astronomical instruments," Opt Express **17**(3), 1947–1962 (2009).
[5] J. Bland-Hawthorn and P. Kern, "Astrophotonics: A new era for astronomical instruments," Opt Express. **17**(3), 1880–1884 (2009).
[6] R. Soref, "Mid-infrared photonics in silicon and germanium," Nature Photonics **4**, 495–497 (2010).
[7] G. Z. Mashanovich, C. J. Mitchell, J. S. Penades *et al.*, "Germanium mid-infrared photonic devices," Journal of Lightwave Technology **35**(4), 624–630 (2017).
[8] A. C. Peacock and N. Healy, "Semiconductor optical fibres for infrared applications: A review," Semiconductor Science and Technology **31**(10), 103004 (2016).
[9] M. Sheik-Bahae, D. J. Hagan, and E. W. V. Stryland, "Dispersion and band-gap scaling the electronic Kerr effect in solids associated with two-photon absorption," Physical Review Letters. **65**(1), 96–99 (1990).
[10] N. K. Hon, R. Soref, and B. Jalali, "The third-order nonlinear optical coefficients of Si, Ge, and Si1-xGex in the midwave and longwave infrared," J Appl Phys. **110**(1) (2011).
[11] J. Ballato, T. Hawkins, P. Foy *et al.*, "Glass-clad single-crystal germanium optical fiber," Optics Express **17**(10), 8029–8035 (2009).
[12] J. Sanghera, L. Shaw, L. Busse *et al.*, "Development and infrared applications of chalcogenide glass optical fibers," Fiber & Integrated Optics. **19**(3), 251–274 (2000).
[13] M. Ordu, J. Guo, B. Tai *et al.*, "Mid-infrared transmission through germanium-core borosilicate glass-clad semiconductor fibers," Optical Materials Express **7**(9), 3107–3115 (2017).
[14] X. Ji, R. L. Page, S. Chaudhuri *et al.*, "Single-crystal germanium core optoelectronic fibers," Advanced Optical Materials **5**(1) (2017).
[15] N. Healy, M. Fokine, Y. Franz *et al.*, "CO2 laser-induced directional recrystallization to produce single crystal silicon-core optical fibers with low loss," Advanced Optical Materials **4**(7), 1004–1008 (2016).
[16] P. Wang, C. Charlton O'Mahony, T. Lee *et al.*, "Mid-infrared Raman sources using spontaneous Raman scattering in germanium core optical fibers," Applied Physics Letters **102**(1), 011111 (2013).
[17] Y. Zhou, S. Constantine, J. A. Gardecki, and L. D. Ziegler, "Dispersed ultrafast nonresonant electronic responses: detuning oscillations and near resonance effects," Chem Phys Lett. **314**(1-2), 73–82 (1999).
[18] J. A. Gardecki, S. Constantine, Y. Zhou, and L. D. Ziegler, "Optical heterodyne detected spectrograms of ultrafast nonresonant electronic responses," J Opt Soc Am B. **17**(4), 652–662 (2000).
[19] B. Fischer, "Theory of self-frequency detuning of oscillations by wave mixing in photorefractive crystals," Optics Letters **11**(4), 236–238 (1986).
[20] S. Mukamel, *Nonlinear Optical Spectroscopy.* (Oxford University Press, New York, NY, 1995).
[21] R. W. Boyd, *Nonlinear Optics*, Third Edition (Academic Press, Burlington, MA, 2008).
[22] P. Hamm and M. Zanni, *Concepts and Methods of 2D Infrared Spectroscopy* (Cambridge University Press, Cambridge UK, 2011).
[23] M. Ordu, J. Guo, B. Tao, J. Bird, S. Ramachandran, and S. N. Basu, Processing and Optical Properties of Ge-Core Fibers. Paper presented at: ICACCJanuary 24-29, 2016; Daytona Beach, Florida, USA.
[24] J. Helbing and P. Hamm, "Compact implementation of Fourier transform two-dimensional IR spectroscopy without phase ambiguity," JOSA B. **28**(1), 171–178 (2011).
[25] P. V. Mamyshev and S. V. Chernikov, "Ultrashort-pulse propagation in optical fibers," Optics Letters **15**(19), 1076–1078 (1990).
[26] G. P. Agarwal, *Nonlinear Fiber Optics*, 5th ed (Academic Press, 2012).